DIGITAL ACCESS TO SCHOLARSHIP AT HARVARD
DASH.HARVARD.EDU

HARVARD LIBRARY
Office for Scholarly Communication

Diverse intracellular pathogens activate Type III Interferon expression from peroxisomes

Citation

Odendall, Charlotte, Evelyn Dixit, Fabrizia Stavru, Helene Bierne, Kate M. Franz, Ann Fiegen, Steeve Boulant, Lee Gehrke, Pascale Cossart, and Jonathan C. Kagan. 2014. "Diverse intracellular pathogens activate Type III Interferon expression from peroxisomes." Nature immunology 15 (8): 717-726. doi:10.1038/ni.2915. http://dx.doi.org/10.1038/ni.2915.

Published Version

doi:10.1038/ni.2915

Permanent link

http://nrs.harvard.edu/urn-3:HUL.InstRepos:14065314

Terms of Use

This article was downloaded from Harvard University's DASH repository, and is made available under the terms and conditions applicable to Other Posted Material, as set forth at http://nrs.harvard.edu/urn-3:HUL.InstRepos:dash.current.terms-of-use#LAA

Share Your Story

The Harvard community has made this article openly available.
Please share how this access benefits you. Submit a story .

Accessibility

NIH Public Access
Author Manuscript
Nat Immunol. Author manuscript; available in PMC 2015 February 01.

Published in final edited form as:
Nat Immunol. 2014 August ; 15(8): 717–726. doi:10.1038/ni.2915.

Diverse intracellular pathogens activate Type III Interferon expression from peroxisomes

Charlotte Odendall[1], **Evelyn Dixit**[1,6], **Fabrizia Stavru**[2,6], **Helene Bierne**[2,5], **Kate M. Franz**[1], **Ann Fiegen**[3], **Steeve Boulant**[4], **Lee Gehrke**[3], **Pascale Cossart**[2], and **Jonathan C. Kagan**[1,*]

[1]Harvard Medical School and Division of Gastroenterology, Boston Children's Hospital, Boston, MA 02115, USA

[2]Institut Pasteur, Unité des Interactions Bactéries Cellules, INSERM U604, INRA USC2020, F-75015, Paris, France

[3]Department of Microbiology and Immunobiology, Harvard Medical School, Boston, Massachusetts 02115, USA, and Institute for Medical Engineering and Science, Massachusetts Institute of Technology, Cambridge MA 02139 USA

[4]CHS Nachwuchsgruppe am Cell Networks Cluster und DKFZ, Department of Infectious Diseases, Virology, University of Heidelberg, Heidelberg 69117, Germany

Abstract

Type I Interferon (IFN) responses are considered the primary means by which viral infections are controlled in mammals. Despite this view, several pathogens activate antiviral responses in the absence of Type I IFNs. The mechanisms controlling Type I IFN-independent responses are undefined. We have found that RIG-I like Receptors (RLRs) induce Type III IFN expression in a variety of human cell types, and identified factors that differentially regulate Type I and III IFN expression. We identified peroxisomes as a primary site that initiates Type III IFN expression, and revealed that the process of intestinal epithelial cell differentiation upregulates peroxisome biogenesis and promotes robust Type III IFN responses in human cells. These findings highlight the interconnections between innate immunity and cell biology.

In mammals, antiviral responses are classically defined as being mediated by Type I Interferons (IFNs). These secreted proteins act via IFN receptors to upregulate IFN-stimulated genes (ISGs) that exhibit diverse antiviral activities[1]. Despite this paradigm, there are several examples of infections that induce ISG expression independently of Type I IFNs[2, 3, 4, 5]. The mechanisms by which these Type I IFN-independent activities are induced

*Correspondence to: jonathan.kagan@childrens.harvard.edu.
[5]Present address: INRA, UMR1319 Micalis, F-78350 Jouy-en-Josas, France, and AgroParis Tech, UMR Micalis, F-78350 Jouy-en-Josas, France
[6]Equal contributions

Author contributions

C.O., E.D., E.F., A.F. and K.M.F. did and analyzed all experiments involving viral infections and peroxisome/mitochondria cell biology; F.S., H.B. and P.C. performed and analyzed all *L. monocytogenes* infection experiments. S.B. prepared and analyzed reovirus stocks. A.F. and L.G. prepared and analyzed DenV stocks. C.O. and J.C.K. wrote the manuscript. All authors edited the manuscript.

Competing financial interests

The authors declare no competing financial interests.

NIH-PA Author Manuscript
NIH-PA Author Manuscript
NIH-PA Author Manuscript

NIH-PA Author Manuscript

NIH-PA Author Manuscript

NIH-PA Author Manuscript

remain unclear. One such example comes from studies of the signaling events mediated by the RIG-I like Receptors (RLRs)[2]. RLRs are RNA helicases that function in virtually all mammalian cells to detect viral and bacterial nucleic acids in the cytosol[6]. The two best-characterized RLRs are RIG-I and Mda5, which differ mainly in their ability to recognize distinct RNA structures. RIG-I detects short double-stranded RNA that contains a 5′ triphosphate group and Mda5 detects long double-stranded RNA structures [6]. These distinct recognition profiles are thought to explain the importance of each RLR in the detection of different classes of viral pathogens[7].

Upon detection of viral RNA, RLRs engage an adaptor protein called MAVS (also known as IPS-1, Cardif or VISA)[8], which is located on the limiting membranes of mitochondria, peroxisomes and mitochondria-associated membranes (MAM) of the endoplasmic reticulum[2, 8, 9]. MAVS engagement by RLRs activates a signaling cascade that induces numerous antiviral activities[10]. Mitochondria-localized MAVS induces an antiviral response typified by the expression of Type I IFNs and ISGs. In contrast, RLR signaling via MAVS on peroxisomes does not induce the expression of any Type I IFN, but does induce ISG expression[2]. This atypical antiviral response is functional, as cells expressing MAVS exclusively on peroxisomes restrict the replication of two mammalian RNA viruses, reovirus and vesicular stomatitis virus (VSV). Thus, while it is clear that Type I IFN-independent mechanisms of antiviral immunity exist, the regulation of these mechanisms remains largely undefined. This lack of information represents a fundamental gap in our knowledge of the means by which mammalian cells respond to intracellular pathogens.

Herein, we report that RLR signaling in human cells can induce the expression of Type III IFNs, a class of IFNs that plays tissue-specific roles in antiviral immunity[11]. We find that RLR-mediated Type III IFN expression can be induced by diverse viruses, including reovirus, sendai virus (SeV) and dengue virus (DenV), as well as the bacterial pathogen *Listeria monocytogenes*. Furthermore, we reveal peroxisomes as signaling organelles that act to induce Type III IFN-mediated ISG responses, which complement the actions of the Type I responses induced from mitochondria. Moreover during the natural process of epithelial cell differentiation and polarization, we observe an increase in the Type III IFN response that correlates with peroxisome abundance, and cells derived from patients with peroxisomal disorders display aberrant antiviral responses. These data establish the importance of peroxisomes in controlling IFN responses, and highlight the interconnectedness of the RLR pathways with the metabolic organelles of mammalian cells.

Results

JAK-STAT-dependent RLR signaling from peroxisomes

Type I IFNs are neither detected nor required for antiviral responses induced by RLRs from peroxisomes[2], suggesting a cell-intrinsic means of antiviral immunity. Cell-intrinsic responses are considered those that do not involve the actions of secreted factors. To determine whether cellular responses induced from peroxisomes induce the secretion of any antiviral factors, we utilized previously characterized MAVS-deficient mouse embryonic fibroblasts (MEFs)[2]. These MEFs stably express MAVS transgenes that were engineered to be localized to single organelles. The resulting isogenic cell populations only differ in that

NIH-PA Author Manuscript

NIH-PA Author Manuscript

NIH-PA Author Manuscript

they display MAVS on either mitochondria (MAVS-mito), peroxisomes (MAVS-pex) or in the cytosol (MAVS-cyto). These cells were infected with mammalian reovirus (a physiological activator of RLRs) and culture supernatants from infected cells were transferred onto Huh7.5 human hepatocyte-like cells. Huh7.5 cells are an Huh7 derivative that carries a loss-of-function mutation in RIG-I[12]. Antiviral activity of the supernatants was then assessed by monitoring the phosphorylation of the transcription factor STAT1. The fact that Huh7.5 cells are deficient for RIG-I signaling ensures that a response would be due to MEF secretion in the supernatant and not carry over virus. Culture supernatants from infected MAVS-pex and MAVS-mito MEFs activated STAT1 phosphorylation (pSTAT1) in Huh7.5 cells (Fig. 1a). In contrast, supernatants from cells expressing the signaling defective 'MAVS-cyto' allele[2, 8] could not trigger pSTAT1, indicating that it did not contain any STAT1 activators. This finding suggested that peroxisomal MAVS can activate cell-extrinsic antiviral responses, despite its inability to induce Type I IFN expression[2].

To determine whether the secreted factor(s) were truly antiviral, the same culture supernatants were allowed to stimulate Huh7.5 cells for 8 hours, at which time the cells were infected with VSV. VSV was chosen for these studies because its ability to replicate is highly sensitive to the actions of IFNs. Compared to supernatants collected from uninfected MEFs, culture supernatants from reovirus-infected MEFs expressing MAVS-pex or MAVS-mito restricted the replication of VSV by 100–1000 fold (Fig. 1b). As expected from the lack of STAT1 phosphorylation, culture supernatants from MAVS-cyto expressing cells exhibited minimal antiviral activity. These results indicate that MAVS signaling from either mitochondria or peroxisomes induces the secretion of antiviral activities that activate STAT1.

To determine whether STAT1 was required for antiviral responses induced from peroxisomes, MAVS-pex expressing MEFs were treated with the small molecule STAT1 inhibitor Fludarabine[13]. In response to reovirus infection, protein expression of the well-characterized ISG viperin was blocked by Fludarabine (Fig. 1c). siRNA based knockdown of STAT1 also revealed a requirement for this transcription factor in the ability of MAVS-pex to induce viperin expression (Fig. 1d and Supplementary Fig. 1a). STAT1 activation is classically governed by Janus Kinases (JAKs)[14]. To determine if JAK signaling was also required for the antiviral responses activated from peroxisomes, we used the pan-JAK inhibitor Pyridone 6 and the JAK2 inhibitors AG490 and 1,2,3,4,5,6-Hexabromocyclohexane (HBC)[15, 16]. All these inhibitors blocked the induction of viperin in response to reovirus in MAVS-pex expressing MEFs (Fig. 1c). siRNA-based knockdown of JAK1 or JAK2 also revealed a requirement for these kinases in the ability of MAVS-pex to induce viperin (also known as *RSAD2*) mRNA expression (Fig. 1e and Supplementary Fig. 1b). Moreover, the pan-JAK inhibitor Pyridone 6 blocked the ability of MAVS-pex expressing MEFs to control VSV replication (Fig. 1f). These data therefore establish that MAVS signaling from peroxisomes induces the secretion of JAK-STAT1 dependent activities, and that these activities are required to create an antiviral cellular state.

NIH-PA Author Manuscript

NIH-PA Author Manuscript

NIH-PA Author Manuscript

RLR-dependent expression and activities of Type III IFNs

The above-described experiments revealed that MAVS signaling from either peroxisomes or mitochondria induce the secretion of antiviral factors. These factors must be cross-reactive between species because MEFs and Huh7 cells are of murine and human origin, respectively. This point is notable because the cellular responses to Type I IFNs are species-specific[17]. For example, recombinant murine IFN-β was unable to restrict VSV replication in human cells (Fig. 1g). Moreover, Type I IFN signaling does not involve JAK2[18], yet JAK2-specific inhibitors (AG490 and HBC) and siRNAs blocked the antiviral actions of this secreted factor (Fig. 1c and 1e). These experiments further verify that signaling from peroxisomal MAVS does not induce the secretion of Type I IFN, and indicate that the secreted factor of interest must be one that crosses species and exhibits antiviral activities that involve JAK2.

While the antiviral activities of Type I IFNs are not able to cross species, those of Type III IFNs are able to do so. For example, recombinant murine Type III IFN (also known as IFN-λ, here IFN-λ2) induced STAT1 phosphorylation (Supplementary Fig. S1c), ISRE activation (Supplementary Fig. S1d) and protection from VSV infection in human cells (Fig. 1g). Murine IFN-β exhibited none of these antiviral activities on human cells (Fig. 1g and Supplementary Fig. 1c, d), as expected[17, 19]. We found that recombinant human IFN-λ1 (but not IFN-β) induced JAK2 phosphorylation (Fig. 1h), as reported[20], and the ability of IFN-λ1 to activate ISRE-based reporter genes was blocked by a pan-JAK inhibitor and by the JAK2-specific inhibitor AG490 (Fig. 1i). Type I IFN signaling was not blocked by AG490 (Fig. 1i). Thus, Type III IFNs exhibit all the properties of the factor secreted after MAVS signaling from peroxisomes.

In contrast to our understanding of Type I IFN gene expression, the mechanisms governing Type III IFN expression are not understood[21]. Type III IFNs (also known as IFN-λs or IL-28 and 29) are produced in response to many viruses, similar to Type I IFNs[11]. Little is known about what differentiates the signaling pathways leading to Type I versus III IFN gene expression, and most studies have focused on the similarities between these two IFN systems[22, 23]. A major hurdle to understanding the regulation of Type III IFN expression is that the most highly inducible family member in humans (IFN-λ1, also known as IL-29) is a pseudogene in mice[24]. Differences in the expression (and function) of the Type III IFN receptor have also been reported when comparing the livers of human and mice[25]. Thus, while the Type III IFN genes are functional in mice, they are less well-expressed and difficult to study experimentally[23, 26]. This difficulty to detect Type III IFN expression has hindered the use of murine models to dissect the signaling pathways that control these antiviral genes. Thus, we used human cells to define the signaling pathways that regulate Type III IFN expression, as humans encode a functional and highly inducible IFN-λ1[11].

We tested the ability of a variety of primary cell types and laboratory cell lines to produce Type I and III IFNs in response to a range of pathogens. We utilized mucosal epithelial and stromal cells of human origin because these cells express the highest levels of the Type III IFN receptor[27], and Type III IFN signaling is required to control infections by mucosal pathogens[28]. We sought to examine encounters between pathogens and the cell types they infect naturally (for example dengue virus in hepatocytes) and also used well-described

NIH-PA Author Manuscript

NIH-PA Author Manuscript

NIH-PA Author Manuscript

activators of the RLR pathway, such as SeV. Infection of primary human hepatocytes, bronchial epithelial cells (BEC), keratinocytes, myoblasts, peripheral blood mononuclear cells (PBMCs) or monocytes with a range of viral pathogens resulted in the coincident expression of IFN-λ1 (*IFNL1*) and IFN-β (*IFNB*) mRNA (Fig. 2a).

In primary cells, IFN-λ basal mRNA levels were far lower than the basal mRNA levels of IFN-β. For this reason, here we did not present the inducible expression of IFN genes as a "fold-induction", but rather as compared to the expression of the housekeeping gene GAPDH. In T84 colonic epithelial cells, Type III IFN expression was induced at least as well as Type I IFN expression in response to reovirus (Fig. 2b). Huh7 hepatocytes also revealed that Type III IFN expression coincides with Type I IFN expression after infection with SeV (Fig. 2c) or DenV (Fig. 2d), the latter being a natural pathogen of hepatocytes[29]. Surprisingly, Huh7 cells did not express any class of IFN genes in response to infection by the bacterial pathogen *L. monocytogenes,* but infection of Jeg3 trophoblasts, a natural target cell type of *Listeria* infections, revealed a strong Type III IFN response (Fig. 2e), consistent with our previous data[30, 31]. These collective data indicate that the expression of Type III IFNs is a common feature of the antimicrobial responses that operate in human cells.

To understand the importance of Type III IFNs in the antiviral activities of human cells, we used neutralizing antibodies to the Type I IFN receptor (IFNAR), the Type III IFN receptor (IFNλR), or a combination of both in T84 intestinal epithelia. At 5h post-infection with reovirus, neutralization of the IFNλR strongly reduced the ability of T84 cells to produce the ISGs viperin or IFIT1 (Fig. 2f). At this time, IFNAR neutralizing antibodies were less effective at influencing ISG expression. 24 hours post-infection, the effectiveness of the neutralizing antibodies was diminished. Nevertheless, the early disruption of ISG expression was functionally important, as Type III IFN signaling was necessary to control reovirus mRNA expression: IFNλR neutralization resulted in more reovirus transcripts as compared to IFNAR neutralization (Fig. 2g). To complement these studies on receptor neutralization, inhibitors of the JAK-STAT pathway were used to determine their effect on ISG expression. Inhibitors of STAT1 (Fludarabine) or JAK2 (AG490) blocked the induction of *VIPERIN* mRNA (Supplementary Fig. S2a) and other ISGs (Fig. 2h) to similar extents, whereas the pan-JAK inhibitor Pyridone-6 nearly abolished ISG expression (Fig. 2h and Supplementary Fig. 2a). Since JAK2 inhibitors only block Type III IFN signaling, these data suggest that Type III IFN signaling controls antiviral gene expression, even when Type I IFNs are expressed.

Common and distinct regulators of IFN-β and IFN-λ

In MEFs, the RLR pathway has been implicated in the control of Type III IFN expression[22]. The aforementioned limitations of the murine system to study Type III IFN expression prompted us to reexamine this question. To investigate the pathway driving Type III IFN expression in human cells, we determined if the RLR-MAVS pathway was required for *IFNL1* mRNA production in response to intracellular pathogens. We chose to use Huh7 cells for these studies, because they are easy to manipulate and are widely used to study host-pathogen interactions. The involvement of RIG-I in Type III IFN signaling was studied using RIG-I deficient Huh7.5 cells[12]. Infection with SeV revealed that RIG-I is required for

NIH-PA Author Manuscript

NIH-PA Author Manuscript

NIH-PA Author Manuscript

IFNL1 as well as *IFNB* mRNA production (Fig. 3a). siRNA-mediated knockdown of MAVS (Supplementary Fig. S2b) also inhibited production of both IFN types in response to SeV (Fig. 3b) and the natural pathogen of hepatocytes, DenV (Fig. 3c)[29]. To determine if MAVS plays a role in bacteria-mediated Type III IFN expression, we infected Jeg3 placental trophoblasts with *L. monocytogenes.* Knockdown experiments (Supplementary Fig. S2c) revealed that MAVS is required for the efficient expression of Type III IFNs, in addition to Type I IFNs during infection by *L. monocytogenes* (Fig. 3d). These collective data indicate that the RLR-MAVS pathway regulates the expression of both classes of IFNs in various human cell types.

To identify proteins in the MAVS pathway that might selectively control Type I or Type III IFN expression, we focused on the most downstream components of the IFN cascade: transcription factors. IFN-β is induced by the combined action of a complex of transcription factors termed the enhanceosome[21]. This involves IRF3 and IRF7, NF-κB and AP-1, the latter of which is activated by MAP kinases (MAPK). The IFN-λ1 promoter contains binding sites for the transcription factors NF-κB and members of the interferon regulatory factor (IRF) family[21]. We used an siRNA-based approach to knock down IRF3 (Supplementary Fig. S2d)[32]. Consistent with its role as a critical regulator of antiviral immunity, IRF3 depletion completely prevented the expression of both classes of IFN in response to SeV and DenV infection (Fig. 3e–f). siRNA-mediated knockdown of IRF7 marginally reduced both type I and III IFN induction to similar extents (Fig. 3g), suggesting that this transcription factor plays a limited role in the production of both cytokines. The IFN-λ promoter also includes 4 NF-κB binding sites. To test the requirement of NF-κB in IFN-λ1 production, we used two small molecule inhibitors: Pyrrolidinedithiocarbamate Ammonium (PDTC) and Bay11 (Fig. 3h–i). Either of these inhibitors blocked SeV-mediated production of *IFNL1* and *IFNB* mRNA with a comparable efficiency, suggesting that NF-κB is also required for the induction of IFN-λ1 in this system. Thus, several common regulatory factors exist that promote the expression of Type I and Type III IFN genes.

In addition to NF-κB and IRF proteins, AP-1 promotes the expression of IFN-β[21]. The AP-1 transcription factor is a large protein complex composed of dimers of members of the c-Jun, c-Fos and ATF families. These complexes are activated by the mitogen activated protein kinases (MAPKs) such as extracellular regulated kinase (ERK), p38 or c-Jun N-terminal kinase (JNK). The role of AP-1 or MAPKs in Type III IFN production is unknown. Small molecule inhibitors of JNK (SP600215), MEK and ERK (PD98059) or p38 (SB202190) were used on Huh7 hepatocytes to assess the role of each MAPK in IFN gene expression in response to SeV infection (Fig. 4a). Whereas p38, JNK or MEK-ERK duo inhibition disrupted *IFNB* mRNA expression to varying extents, only p38 inhibitors disrupted *IFNL1* mRNA expression (Fig. 4a). Treatment with JNK or MEK-ERK duo inhibitors did not interfere with Type III IFN expression (Fig. 4a). siRNA-based knockdowns ERK family members confirmed their selective role in the expression of *IFNB mRNA* (Fig. 4b and Supplementary Fig 2e). p38 siRNAs differed from the results obtained with inhibitors, and suggested a selective role for this MAPK family in IFN-β expression (Fig. 4c, Supplementary Fig 2f). These data indicate that each component of the enhanceosome is necessary for *IFNB* gene expression, but a subset of enhanceosome components are

NIH-PA Author Manuscript

NIH-PA Author Manuscript

NIH-PA Author Manuscript

sufficient for *IFNL1* mRNA expression. Thus, it stands to reason that distinct signaling pathways may exist that selectively promote the expression of Type III IFN genes without activating the expression of Type I IFNs.

The above data revealed that some MAPKs are selectively needed for the expression of Type I IFNs. To determine if factors exist that are selectively needed for Type III IFN expression, we considered the transcription factor IRF1. Although IRF1 is an ISG, it is present in a variety of cells prior to viral infection[33] (Supplementary Fig. 2g). IRF1 was the first IRF family member shown to bind the *IFNB* promoter[33], suggesting an important role in regulating expression of this gene. However, IRF1 was later demonstrated to be dispensable for Type I IFN expression during viral infections of *Irf1* deficient MEFs or mice[34]. IRF1 was also implicated in Type I IFN-independent antiviral responses[2, 35], perhaps via interactions with the *IFNL1* promoter in the lung[36, 37]. We used siRNA-based approaches to define the role of IRF1 in the regulation of IFN expression. RNAi-mediated knockdown of IRF1 was carried out in Huh7 cells (Supplementary Fig. S2g), which were subsequently infected with SeV. IRF1 knockdown had no effect on *IFNB* mRNA levels at 6h post infection (Fig. 4d, top left panel). However, IRF1 knockdown completely inhibited the expression of *IFNL1* mRNA after SeV infection (Fig. 4d, bottom panels). These data reveal an important role for IRF1 in controlling Type III IFN expression.

At late time points of infection (24h), IRF1 seemed to be involved in the production of both classes of IFNs (Fig. 4d, right hand panels). However, at these time points, the synergistic effects of secreted IFNs and RLR signaling may complicate our ability to explain this observation. A useful means to further address the role of IRF1 in IFN expression would be to study a virus that prevents signaling induced by secreted IFNs. DenV is useful in this regard, as this virus blocks signaling downstream of IFN receptor ligation[38]. Although IRF1 was not required for *IFNB* expression in response to DenV, it promoted *IFNL1* mRNA expression (Fig. 4e). Since both IRF1 and IRF3 regulate *IFNL1* mRNA expression, we considered the possibility that IRF1 might somehow regulate the activation of IRF3. This was assessed by determining if IRF3 can be phosphorylated in Huh7 cells that have been depleted of IRF1 through the use of siRNAs. We found that SeV infection induced the phosphorylation of IRF3 within 3 hours of infection, even when IRF1 was knocked down (Fig. 4f). This result suggests that IRF1 and IRF3 are activated independently of each other, but act together to promote the expression of *IFNL1* mRNA. Overall, these data reveal an important role for IRF1 in the control of Type III IFN expression induced by multiple viral pathogens, especially during the primary phase of infection. Thus, IRF1 can be considered a counter to ERK, in that it is selectively required for Type III IFN expression, whereas ERK is selectively required for Type I IFN expression. Taken together these data demonstrate that many common regulators control Type I and III IFN expression, but these genes can also be expressed independently of each other.

Peroxisomal MAVS induces the selective expression of IFN-λ

We have shown above that peroxisomal MAVS induces the secretion of a factor that can cross species to activate a JAK-STAT pathway that is regulated by JAK2. We also showed that human Type III IFN signaling is regulated by JAK2, but Type I IFN signaling is not.

NIH-PA Author Manuscript

NIH-PA Author Manuscript

NIH-PA Author Manuscript

These results suggest that peroxisomal MAVS preferentially induces Type III IFNs. To test this prediction directly, a cell type was needed that expressed high levels of Type III IFNs and expressed MAVS selectively on peroxisomes. Huh7 cells were therefore engineered to stably express the relocalized MAVS transgenes described above and elsewhere[2]. These transgenes encode either wild type (WT) MAVS or mutants that are localized specifically to mitochondria, peroxisomes or the cytosol. The resulting cell populations were flow sorted to select clones that express comparable amounts of the transgenes (Supplementary Fig 2h). The endogenous MAVS mRNA was then depleted through the use of siRNAs that target the 5′ untranslated region of the MAVS mRNA, resulting in cell lines that preferentially expressed the transgene of interest. To test whether peroxisomal MAVS in human cells was able to induce STAT1 phosphorylation in a JAK2-dependent manner, cells were treated with the pan-JAK inhibitor Pyridone 6 and the JAK2 inhibitors AG490 and HBC. SeV infection induced STAT1 phosphorylation in the cells expressing the WT MAVS, MAVS-pex or MAVS-mito alleles (Fig. 5a). This response was blocked by all the inhibitors listed above, indicating that MAVS-pex Huh7 cells respond similarly to MAVS-pex MEFs, and can be used to test whether MAVS localized on peroxisomes induces Type III IFN expression. We noted that a weak phospho-STAT1 signal was induced by SeV in cells expressing the signaling-deficient MAVS-cyto allele, probably resulting from incomplete MAVS knockdown (Fig. 5a). This observation highlights some limitations of this system, but also the importance of this negative control in the experiments that follow. Indeed, we found some residual SeV-mediated IFN production in the MAVS-cyto expressing cells (Fig. 5b). Therefore, IFN levels produced by the MAVS-cyto line were used to draw a ‘background’ line, above which signaling was considered significant. In response to SeV infection, only WT and MAVS-mito alleles induced the expression of *IFNB* mRNA, whereas MAVS-pex cells did not (Fig. 5b). However, MAVS-pex induced the expression of *IFNL1* mRNA (Fig. 5b). Infection with DenV (Fig. 5c) yielded comparable results—peroxisomal MAVS induced *IFNL1*, but not *IFNB* mRNA, whereas WT and mitochondrial MAVS were able to induce both. The magnitude and kinetics of each transcriptional response differed greatly between viral infections, a result that likely reflects some aspect of the diverse lifecycles of the pathogens examined.

To determine if the ability of peroxisomal MAVS to induce Type III IFN expression extended to bacterial infections, we returned to *L. monocytogenes* and Jeg3 cells, in which MAVS transgenes were overexpressed (Supplementary Fig 2i). Since infection with this bacterium disrupts mitochondria[39], and mitochondrial disruption hinders RLR signaling from this organelle[40], we hypothesized that peroxisomal MAVS might play a dominant role in the IFN response to *L. monocytogenes* infection. Indeed, in Jeg3 trophoblasts, where the IFN response to *L. monocytogenes* is MAVS-dependent (Fig. 3d), expression of peroxisomal MAVS strongly potentiated the ability of these cells to express *IFNL1*, although *IFNB* mRNA was also induced (Fig. 5e). Overexpression of MAVS-mito did not induce the expression of any class of IFN above MAVS-cyto levels (Fig. 5e). The observation that peroxisomal MAVS contributes to Type I IFN expression during *L. monocytogenes* infection, but not during viral infection, is noteworthy. One potential explanation for this finding is based on the fact that in addition to RLRs, *L. monocytogenes* activates transcription-inducing NOD-like Receptors (NLRs) and other Pattern Recognition Receptors

NIH-PA Author Manuscript

NIH-PA Author Manuscript

NIH-PA Author Manuscript

(PRRs) in the cytosol[41]. The transcription factors activated by RLRs and other PRRs may synergize to create a transcriptional profile distinct from that seen for viruses that only activate RLRs.

Although the above experiments revealed the ability of peroxisomal MAVS to induce the selective expression of Type III IFNs, the magnitude of IFN and ISG expression was less than that observed for cells expressing WT MAVS. This result is consistent with prior work showing that MAVS signaling from peroxisomes and mitochondria (coordinated around the MAM) synergize to induce maximal expression of antiviral genes[2, 9]. To determine whether the amount of IFNs released by cells expressing MAVS-pex was functional, we asked if culture supernatants from infected cells could confer an antiviral state. Culture supernatants from infected MAVS-pex Huh7 cells were transferred onto Huh7.5 cells, and the ability of VSV to replicate was assessed. In response to either SeV (Fig. 5f, left panel) or DenV (Fig. 5f, right panel), peroxisomal MAVS induced the release of functional amounts of IFNs that blocked VSV replication. Collectively, these data establish peroxisomes as an organelle that can induce the selective expression of Type III IFNs upon RLR-MAVS pathway activation.

To determine if the pathway leading from peroxisomal MAVS was similar to that observed in WT cells, the effect of MAPK inhibitors on virus-induced gene expression was assessed. Whereas WT MAVS signaling was inhibited by the JNK (SP600125), MEK and ERK (PD98059), and p38 (SB202190) inhibitors, *VIPERIN* mRNA production in the Huh7 cells expressing MAVS-pex was unaffected (Fig. 5g). siRNA-based knock-down of ERK in MEFs also abolished the ability of SeV to induce STAT1 phosphorylation upon signaling by WT MAVS, but not MAVS-pex (Fig. 5h and Supplementary Fig 2j), further confirming that this MAPK does not control Type III IFN responses.

Peroxisome abundance controls the production of IFN-λ

Although the Type I IFN system appears to be important in most mammalian cell types, the Type III IFNs appear to be most critical at mucosal surfaces, in particular in epithelial cells of the intestine, liver and lung. These observations suggest that epithelial cells might exhibit unusual cell biological characteristics that enhance the Type III IFN system. To address this possibility, we turned our attention to human T84 intestinal epithelial cells, which can be differentiated into a polarized monolayer of cells that exhibit many functional and morphological properties of primary epithelia. T84 differentiation occurs over the course of several days, thus allowing us to determine if the process of epithelial differentiation into a polarized monolayer would influence the RLR-MAVS pathway. As expected, the transepithelial resistance of the T84 monolayer increased over time, which is a functional indication of epithelial polarization (Fig. 6a). As T84 intestinal epithelial cells polarized, the abundance of peroxisomes increased, whereas mitochondria remained unchanged (Fig. 6b and Supplementary Fig 3). This increase in peroxisome abundance correlated with an increase in the expression of the Pex11β gene (*PEX11B*), which is a master regulator of peroxisome proliferation (Fig. 6c). To determine if the change in the abundance of peroxisomes relative to mitochondria influences RLR-MAVS signaling events, the T84 cells were infected with the intestinal pathogen reovirus at various times during the differentiation process. At any day of differentiation, the T84 cells responded equally well to reovirus and

NIH-PA Author Manuscript

NIH-PA Author Manuscript

NIH-PA Author Manuscript

produced roughly equal levels of *IFNB* mRNA (Fig. 6d). In contrast, the magnitude of the IFN-λ response (*IFNL1* mRNA levels) increased over time (Fig. 6d and 6e), which correlated with an increase in *PEX11B* mRNA, peroxisome abundance and transepithelial resistance. These data reveal that as epithelial cells differentiate into a polarized monolayer, they shift from a dominant Type I IFN to Type III IFN response, which may be caused by an increase in peroxisome abundance.

To determine if increasing peroxisome abundance was sufficient to influence the RLR-MAVS pathways, we induced the proliferation of peroxisomes in Huh7 cells by overexpression of aforementioned regulator of peroxisome biogenesis, Pex11β. As expected[42], we observed a significant increase of Pex14-positive peroxisomes in Pex11β-expressing cells (Fig. 6f). This increase in peroxisome abundance correlated with an increase in *IFNL1* mRNA production in response to SeV infection, but *IFNB* mRNA was unaffected (Fig. 6g). These data therefore provide a direct link between the abundance of peroxisomes and the quality of the IFN response induced by the RLR-MAVS pathway.

Finally, we sought to determine whether the endogenous MAVS protein on peroxisomes was sufficient to induce Type III IFNs. Disruption of mitochondrial function with the protonophore carbonyl cyanide m-chlorophenylhydrazone (CCCP) has been used to reveal the importance of mitochondrial integrity for RLR signaling[40]. Notably, peroxisome functions are unaffected by CCCP[43]. We reasoned that if endogenous peroxisome-localized MAVS functioned to control Type III IFN expression, then CCCP-treated cells may retain the ability to induce these IFNs. Alternatively, if mitochondria are the sole subcellular site of RLR-MAVS signaling, then CCCP treatment should block the expression of all RLR-induced genes to similar extents. To address this possibility, primary human keratinocytes were used because they produce and respond to Type III IFNs and because they tolerate CCCP treatment. Over the course of the 3 day experiments, keratinocytes remained viable and robust. CCCP treatment eradicated the functional mitochondrial pool in these cells, as assessed by mitotracker staining (Fig. 6h). Under these conditions, SeV-mediated *IFNB* mRNA production was completely inhibited (Fig. 6i), similar to what was observed[40]. By contrast, expression of the ISG viperin and *IFNL1* was enhanced in the presence of CCCP (Fig. 6i). These data indicate that even within primary cells, the endogenous RLR signaling pathway can operate in the absence of functional mitochondria, and that this pathway can be ‘rewired’ to produce only Type III IFNs, likely from peroxisomes.

Zellweger cells implicate peroxisomes in RLR signaling

The studies described above suggested that RLR signaling via MAVS can occur in cells lacking functional mitochondria, thus raising the question of how MAVS populates peroxisomes and how these organelles are functionally interconnected. To address these questions, we employed cells derived from human patients with Zellweger syndrome, which is a peroxisome biogenesis disorder (PBD). PBD patients have defective peroxisomes and suffer from various developmental abnormalities, which often results in death early in life[44]. Death can be associated with infection (usually pneumonia) and patients display elevated cytokine levels, particularly in the brain[45]. The immunological basis for these observations

NIH-PA Author Manuscript

NIH-PA Author Manuscript

NIH-PA Author Manuscript

is unclear, as Zellweger disease cells have not been thoroughly examined for alterations in innate immune signaling pathways.

Zellweger cells that lack a functional *PEX14* gene contain peroxisomal membranes that stain for the membrane protein PMP70, but these organelles lack all cargo that is normally present in the lumen, such as catalase[44] (Supplementary Fig. S4). We found that cells lacking Pex14 retain MAVS on their limiting membrane (Supplementary Fig. S5), suggesting that MAVS does not require Pex14 for its ability to localize to peroxisomes. Thus, MAVS can be categorized as a peroxisomal membrane protein that is targeted to these organelles by Pex14-independent means.

Unlike the Pex14-deficiency, Zellweger patients that lack functional Pex16 or Pex19 lack physically distinct peroxisomes[46] (see also Supplementary Fig. S4). Interestingly, in these cells, peroxisomal membrane proteins can be mistargeted to mitochondria[47, 48]. Thus, Pex19- or Pex16-deficient cells contain mitochondria that display both peroxisomal and mitochondrial proteins on their limiting membranes. These observations are intriguing when considering recent work suggesting that physical interactions between mitochondria and peroxisomes lead to an enhanced RLR-dependent response to viral infection[9]. Although the molecular basis for these observations remain unclear, it seems reasonable that membrane proteins on each organelle would interact to promote more efficient MAVS-dependent cellular responses. For this reason, we wondered if Zellweger cells lacking Pex19, which contain peroxisomal and mitochondrial proteins on the same organelle, might display an aberrant response to viral infection. To address this possibility, we infected Pex19-deficient cells or Pex19-deficient cells stably expressing Pex19 with mammalian reovirus. The cells were then examined 9 and 16 hours post infection by microarray analysis. Reovirus infection of both genotypes induces a gene expression profile typical for an antiviral immune response, as apparent from GO-term analysis (Supplementary Fig. S6a). Global transcriptome analysis revealed that Pex19 deficient cells displayed a higher antiviral response at all time points examined (Supplementary Fig. S6b–d). Of note, of the 20 genes that are most highly upregulated in Pex19 deficient cells compared to reconstituted cells, most are ISGs (Supplementary Fig. S6d). These data suggest that the presence of mitochondria containing peroxisomal proteins promotes greater RLR-dependent responses. These studies underscore the important role of peroxisomes in regulating RLR signaling, and provide the first insight in immunological consequences of Pex19 deficiency in human disease.

Discussion

The data presented in this study demonstrate that RLRs can signal via MAVS from peroxisomes to drive the synthesis of Type III IFNs. Most notably, we reveal that the RLR pathway can induce the expression of different classes of IFN genes, and the decision of which genes to induce is determined by the location in the cell where RLR signaling is initiated. This study therefore highlights how the microenvironments of different cell types can influence the activity of a given signaling pathway. Several lines of evidence support these conclusions. First, using both direct (mRNA quantification) and indirect (functional assays) approaches, we found that the RLR network can induce the expression of Type I and

NIH-PA Author Manuscript

NIH-PA Author Manuscript

NIH-PA Author Manuscript

Type III IFNs in response to infections with diverse intracellular pathogens. These results were obtained in 7 primary human cell types and 3 different cell lines. Second, the ability of Type III IFNs to be expressed is directly controlled by the differentiation state of intestinal epithelial cells, and appears to occur as a function of the abundance of peroxisomes. Third, depletion of mitochondria in primary human keratinocytes does not inactivate the RLR pathway, but rather shifts the RLR pathway to be a primary producer of Type III IFNs. These collective data identify Type III IFNs are a major component of the RLR pathway emanating from peroxisomes, and suggest that cell-type specific expression of classes of IFNs can be achieved by altering the abundance of peroxisomes or mitochondria in a given cell population.

It has been generally considered that Type I and Type III IFN expression is co-regulated and induced by a common (unknown) signaling pathway. Our work to define the means by which peroxisomal MAVS can induce antiviral gene expression revealed that these IFN classes can be induced differentially. We identify the existence of complementary but distinct sets of regulators that control Type I and Type III IFN expression. Most notably, we find that the transcription factor IRF1 is necessary for Type III IFN expression and ERK MAPKs are necessary for Type I IFN expression. These data suggest a plausible model whereby Type III IFN expression from peroxisomes can be achieved without the expression of Type I IFNs. We suggest that the MAVS pathway from peroxisomes does not activate ERK, but does activate NF-κB and IRF3. This partial activation of the components of the classically defined enhanceosome would preclude the expression of *IFNB*, but would permit the expression of *IFNL* genes. When considered in this context, it would be expected that pathogens that activate multiple pattern recognition receptors may create a means of ‘complementing’ the defect in MAPK signaling and allow the peroxisomal pathway to induce Type I IFN expression. This idea may therefore explain why peroxisomal MAVS induces the expression of Type I and Type III IFN during *Listeria* infections, as these bacteria also strongly activate MAPK family members.

Although our studies highlight how Type III IFNs can be induced selectively from peroxisomes in epithelial cells, they also raise the question of why these different IFN families exist. One would expect that Type III IFNs would induce different cellular responses than their Type I counterparts. However, gene expression analysis has indicated a largely overlapping set of genes that are induced by the Type I and Type III IFN receptors. Why then is the expression of the Type III IFN receptor selectively detected on mucosal epithelial cells, and why is the ability of intestinal epithelia to express Type III IFNs dependent on the degree of cell polarization? We propose that the RLR pathway (via Type III IFNs) may elicit non-transcriptional cellular responses that are more compatible with the specific homeostatic functions of epithelia than RLR-induced Type I IFNs. Possible examples of such cellular responses include activities that may influence cell-cell communication, viability or metabolism. This prediction may explain why Type III IFN expression is linked to the polarization of T84 intestinal epithelial cells, and may explain the benefit of allowing RLR signaling to occur from multiple organelles. By separating the subcellular sites of RLR signaling, and allowing different cellular responses to occur from these different sites, the RLR network can be modified to emphasize or de-emphasize an

NIH-PA Author Manuscript

NIH-PA Author Manuscript

NIH-PA Author Manuscript

organelle-specific response to fit the homeostatic needs of any given type of cell. The findings presented in this study support these ideas and provide a mandate for future work on the cell-type specific functions of the innate immune signaling networks in mammals.

Methods

Plasmids, antibodies, siRNAs and recombinant proteins

Chimeric MAVS alleles were described respectively[1]. Pex13-GFP and Myc-Pex11 was obtained from Marc Fransen. Anti-viperin, MAVS, phospho STAT1, GFP, PMP70, catalase, mitochondrial HSP70, tubulin and actin antibodies were obtained from Biolegend (Cat #97736), Bethyl labs (A300-782A), BD Transduction (Cat # 612132, Clone 14/P-STAT1), Clontech (Cat# 632380) or Invitrogen (Cat# 11122), Sigma (Cat# SAB4200181), Santa Cruz (Cat# sc-34280), Thermo (Cat# MA3-028, Clone JG1), Sigma (Cat# T6074) and Sigma (Cat # A5441, Clone AC-15) respectively. Antibodies to STAT1, phospho IRF3, phospho JAK2, JAK2, IRF1 were obtained from BD Transductions (Cat# 610115, Clone 1/Stat1), Cell Signaling (Cat# 4947), Santa Cruz (Cat# sc16566), Santa Cruz (Cat# sc278, Clone HR-758), Cell Signaling (Cat# 8478, Clone D5E4), respectively. Anti-Pex14 was obtained from Marc Fransen. Taking advantage of the high concentration of biotin dependent carboxylases in mitochondria, Streptavidin-Alexa488 was used to label mitochondria[2]. IRF1 and IRF3 siRNAs were obtained from Ambion with the respective sequences CCAGUGAUCUGUACAACU and ACAUAAAAUCUACGAGUU. siRNAs targeting MAVS and IRF7 in Huh7 cells was obtained from Qiagen with the following sequences AACGACUUCUGUUCUGGAUAU, CCCGAGCTGACGTTCCTATA . siRNA targeting MAVS in JEG3 cells (CCGUUUGCUGAAGACAAGA) was obtained from MWG Operon. siRNAs to mouse JAK1 (TACCAGGATGCGAATAAATAA), mouse JAK2 (ATGATTGGCAATGATAAACAA), human ERK1 (CCGGCCCATCTTCCCTGGCAA), human ERK2 (AACAAAGTTCGAGTAGCTATC) were obtained from Qiagen. siRNAs to human ERK1 (ID 77117) and 2 (ID 77106), and mouse STAT1 (ID 74445)were obtained from Ambion. siRNA to human p38 was obtained from Cell signaling (cat #6564).

Cell lines, retroviral gene transfer and transfections

MEFs, Huh7 and Jeg3 cells were cultured according to standard techniques. 293T ISRE Luciferase cells were obtained from Nir Hacohen (Harvard). T84 epithelial cells were cultured and polarized as previously described[3]. Primary human foreskin keratinocytes were a gift from Karl Munger and were isolated from anonymous newborn circumcisions and cultured as previously described[4]. Primary human hepatocytes and bronchial epithelial cells were obtained from Lonza and cultured according the manufacturer's recommendations. Primary myoblasts were obtained from Mytogen and cultured and infected as described[5]. Blood of healthy individuals was collected and PBMCs were isolated using Lympholyte and SepMate columns or Ficoll gradient. Monocyte were further purified using EasySep beads (StemCell Technologies). Pex14 and Pex16 deficient human skin fibroblasts were obtained from Marc Fransen. Pex19 deficient and reconstituted human skin fibroblasts as well as MEFs expressing chimeric MAVS alleles were described[1]. The same chimeric MAVS alleles were introduced in Huh7 cells and then sorted for equal GFP florescence to normalize MAVS expression levels. Where indicated, Huh7 cells were transfected with 40

NIH-PA Author Manuscript

NIH-PA Author Manuscript

NIH-PA Author Manuscript

nM siRNA oligos using JetPRIME (Polyplus transfections) for 48h. Knockdown in Jeg3 cells was carried out with 30 nM siRNA using Lipofectamine RNAiMAX (Invitrogen). Protein knockdown was determined by western immunoblotting using standard techniques or RT-qPCR, as described below. Transient DNA transfections in Jeg3 cells were carried out with 0.5 μg DNA/cm^2 using Fugene HD (Promega), following the manufacturer's recommendations.

Virus stocks, bacterial strains and infections

Reovirus Type 3 Dearing Cashdollar was propagated in L929 cells and plaque purified as described[6]. SeV was obtained from Charles River labs. Dengue 2 virus strain New Guinea C was isolated from a febrile patient in the 1940s[7], and was propagated on C6-36 mosquito cells cultured in RPMI (Gibco) at 28C, 5% CO2. Infectious C6-36 supernatant was titered by flow cytometry[8]. *Listeria monocytogenes* EGD strain (BUG600) was described previously[9]. Cells were seeded 16–24h before infection or transfection. On the day of the infection, medium was replaced with serum free medium containing virions at multiplicities of infection of 1 (DenV) or 100 (Reo) or 50 HAU/ml (SeV). *Listeria monocytogenes* infections were carried out at an MOI of 0.1, as described[10].

Inhibitors and microscopy

With exception of Fludarabine, obtained from Tocris Biosciences and CCCP obtained from Sigma, all inhibitors were obtained from Calbiochem. Cells were incubated with 10–50 μM Fludarabine, 2 μM Pyridone 6, 10–50 μM AG490, 10–100 μM 1,2,3,4,5,6-Hexabromocyclohexane (JAK2 inhibitor II, HBC), 5 μM Bay11, 50 μM PDTC, 30 μM PD98059, 100 μM SP600125, 10 μM SB202190 for 30 min, prior to infection or treatment. In case of IFN treatment, cells were incubated in fresh medium with 0.01 μg/ml human IFN-λ1 or mouse IFN-λ2 (Peprotech), 10 U/ml human IFN-β or 50 U/ml mouse IFN-β (PFL Interferon Source) for 2–5h. Keratinocytes were incubated in media containing either 10 μM CCCP or DMSO. Cells were incubated for 48 hours and then infected or incubated with 250 nM MitoTracker Deep Red FM (Molecular Probes) for 30 min at 37°C prior to fixation in 2% paraformaldehyde in PBS. Confocal images were acquired using a spinning disk confocal head (CSU-X1, Perkin Elmer Co., Boston, MA) coupled to a fully-motorized inverted Zeiss Axiovert 200M microscope equipped with a 63X lens (Pan Apochromat, 1.4 NA). The imaging system operates under control of SlideBook 5 (Intelligent Imaging Innovations Inc, Denver, CO). Micrographs were processed with Adobe Photoshop.

mRNA detection, nCounter analysis and gene arrays

Cells were lysed in RLT buffer (Qiagen) supplemented with β-Mercaptoethanol, and passed through Qiashredder columns (Qiagen). RNA was then isolated using RNeasy columns (Qiagen) following the manufacturer's recommendations. RT-qPCR was carried out with a Bio-Rad iQ5 or CFX384 real time cycler with Taqman probes as directed by the manufacturer. nCounter CodeSets were constructed to detect genes selected by the Gene-Selector algorithm and additional controls as described[11]. Purified RNA was hybridized for 16 hr with the CodeSet and loaded onto the nCounter prep station, followed by quantification with the nCounter Digital Analyzer. To allow for side-by-side comparisons of

NIH-PA Author Manuscript

NIH-PA Author Manuscript

NIH-PA Author Manuscript

nCounter experiments, we normalized the nCounter data in two steps. We first controlled for small variations in the efficiency of processing by normalizing measurements from all samples analyzed on a given run to the levels of chosen positive controls provided by the nCounter instrument. Second, we normalized the data obtained for each sample to the expression of a control gene (GAPDH). These genes were described to be unchanged in cells exposed to a variety of infectious conditions[11]. For every sample, we computed the weighted average of the mRNA counts of the control transcript and normalized the sample's values by multiplying each transcript count by the weighted average of the controls.

Microarrays were performed by the Molecular Genetics Core Facility at Boston Children's Hospital supported by NIH-P50-NS40828 and NIH-P30-HD18655. Quantile normalization was used for signal extraction and normalization. For comparison of gene expression profiles between genotypes and time points log-transformed data was plotted and a weighted linear fit calculated. For gene ontology analysis p-values were calculated using the hypergeometric distribution and adjusted for multiple hypotheses testing by Holm's method. Microarray data sets are available through the Gene Expression Omnibus (GEO); accession number GSE56783.

Statistics

GraphPad Prism was used for all statistical analyses. Statistical analysis was carried out by one-way analysis of variance (ANOVA) followed by Dunnett's test or unpaired student's *t*-test (two-tailed). $P < 0.05$ was considered statistically significant. No pre-experiment statistical methods, randomization or blinding were used. Sample-size choice and assumption of normality were based on similar analyses in published studies.

Supplementary Material

Refer to Web version on PubMed Central for supplementary material.

Acknowledgments

We would like to thank the members of the Kagan lab for helpful discussions. We would like to thank Marc Fransen for providing cell tines and reagents and Bradlee Nelms for bioinformatic assistance. J.C.K. is supported by NIH grants AI093589, AI072955 and P30 DK34854, and an unrestricted gift from Mead Johnson & Company. Dr. Kagan holds an Investigators in the Pathogenesis of Infectious Disease Award from the Burroughs Wellcome Fund. CO is supported by a fellowship from the Crohn's and Colitis Foundation of America. E.D. is supported by an Erwin Schrödinger Fellowship of the Austrian Science Fund (FWF). K.M.F. is supported through the Herchel Smith Graduate Fellowship Program. L.G. and J.C. K are supported by a MIT-BCH Collaborative grant, and L.G. is supported by NIH grant CA159132. P.C. is supported by ERC Advanced Grant 233348 MODELIST and is an HHMI senior international research scholar.

References

1. Takeuchi O, Akira S. Innate immunity to virus infection. Immunological reviews. 2009; 227(1):75–86. [PubMed: 19120477]
2. Dixit E, Boulant S, Zhang Y, Lee AS, Odendall C, Shum B, et al. Peroxisomes are signaling platforms for antiviral innate immunity. Cell. 2010; 141(4):668–681. [PubMed: 20451243]
3. Noyce RS, Collins SE, Mossman KL. Identification of a novel pathway essential for the immediate-early, interferon-independent antiviral response to enveloped virions. Journal of virology. 2006; 80(1):226–235. [PubMed: 16352547]

NIH-PA Author Manuscript

NIH-PA Author Manuscript

NIH-PA Author Manuscript

4. Noyce RS, Taylor K, Ciechonska M, Collins SE, Duncan R, Mossman KL. Membrane perturbation elicits an IRF3-dependent, interferon-independent antiviral response. Journal of virology. 2011; 85(20):10926–10931. [PubMed: 21813605]
5. Peltier DC, Lazear HM, Farmer JR, Diamond MS, Miller DJ. Neurotropic arboviruses induce interferon regulatory factor 3-mediated neuronal responses that are cytoprotective, interferon independent, and inhibited by Western equine encephalitis virus capsid. Journal of virology. 2013; 87(3):1821–1833. [PubMed: 23192868]
6. Nakhaei P, Genin P, Civas A, Hiscott J. RIG-I-like receptors: sensing and responding to RNA virus infection. Seminars in immunology. 2009; 21(4):215–222. [PubMed: 19539500]
7. Kato H, Takeuchi O, Sato S, Yoneyama M, Yamamoto M, Matsui K, et al. Differential roles of MDA5 and RIG-I helicases in the recognition of RNA viruses. Nature. 2006; 441(7089):101–105. [PubMed: 16625202]
8. Seth RB, Sun L, Ea CK, Chen ZJ. Identification and characterization of MAVS, a mitochondrial antiviral signaling protein that activates NF-kappaB and IRF 3. Cell. 2005; 122(5):669–682. [PubMed: 16125763]
9. Horner SM, Liu HM, Park HS, Briley J, Gale M Jr. Mitochondrial-associated endoplasmic reticulum membranes (MAM) form innate immune synapses and are targeted by hepatitis C virus. Proceedings of the National Academy of Sciences of the United States of America. 2011; 108(35): 14590–14595. [PubMed: 21844353]
10. Belgnaoui SM, Paz S, Hiscott J. Orchestrating the interferon antiviral response through the mitochondrial antiviral signaling (MAVS) adapter. Current opinion in immunology. 2011; 23(5): 564–572. [PubMed: 21865020]
11. Kotenko SV. IFN-lambdas. Current opinion in immunology. 2011; 23(5):583–590. [PubMed: 21840693]
12. Sumpter R Jr, Loo YM, Foy E, Li K, Yoneyama M, Fujita T, et al. Regulating intracellular antiviral defense and permissiveness to hepatitis C virus RNA replication through a cellular RNA helicase, RIG-I. Journal of virology. 2005; 79 (5):2689–2699. [PubMed: 15708988]
13. Frank DA, Mahajan S, Ritz J. Fludarabine-induced immunosuppression is associated with inhibition of STAT1 signaling. Nature medicine. 1999; 5(4):444–447.
14. Stark GR, Darnell JE Jr. The JAK-STAT pathway at twenty. Immunity. 2012; 36 (4):503–514. [PubMed: 22520844]
15. Meydan N, Grunberger T, Dadi H, Shahar M, Arpaia E, Lapidot Z, et al. Inhibition of acute lymphoblastic leukaemia by a Jak-2 inhibitor. Nature. 1996; 379(6566):645–648. [PubMed: 8628398]
16. Sandberg EM, Ma X, He K, Frank SJ, Ostrov DA, Sayeski PP. Identification of 1,2,3,4,5,6-hexabromocyclohexane as a small molecule inhibitor of jak2 tyrosine kinase autophosphorylation [correction of autophophorylation]. Journal of medicinal chemistry. 2005; 48(7):2526–2533. [PubMed: 15801842]
17. Veomett MJ, Veomett GE. Species specificity of interferon action: maintenance and establishment of the antiviral state in the presence of a heterospecific nucleus. Journal of virology. 1979; 31(3): 785–794. [PubMed: 513194]
18. Watling D, Guschin D, Muller M, Silvennoinen O, Witthuhn BA, Quelle FW, et al. Complementation by the protein tyrosine kinase JAK2 of a mutant cell line defective in the interferon-gamma signal transduction pathway. Nature. 1993; 366(6451):166–170. [PubMed: 7901766]
19. Berger Rentsch M, Zimmer G. A vesicular stomatitis virus replicon-based bioassay for the rapid and sensitive determination of multi-species type I interferon. PloS one. 2011; 6(10):e25858. [PubMed: 21998709]
20. Lee SJ, Kim WJ, Moon SK. Role of the p38 MAPK signaling pathway in mediating interleukin-28A-induced migration of UMUC-3 cells. International journal of molecular medicine. 2012; 30(4):945–952. [PubMed: 22825757]
21. Iversen MB, Paludan SR. Mechanisms of type III interferon expression. Journal of interferon & cytokine research : the official journal of the International Society for Interferon and Cytokine Research. 2010; 30(8):573–578.

NIH-PA Author Manuscript

NIH-PA Author Manuscript

NIH-PA Author Manuscript

22. Onoguchi K, Yoneyama M, Takemura A, Akira S, Taniguchi T, Namiki H, et al. Viral infections activate types I and III interferon genes through a common mechanism. The Journal of biological chemistry. 2007; 282(10):7576–7581. [PubMed: 17204473]
23. Osterlund PI, Pietila TE, Veckman V, Kotenko SV, Julkunen I. IFN regulatory factor family members differentially regulate the expression of type III IFN (IFN-lambda) genes. J Immunol. 2007; 179(6):3434–3442. [PubMed: 17785777]
24. Lasfar A, Lewis-Antes A, Smirnov SV, Anantha S, Abushahba W, Tian B, et al. Characterization of the mouse IFN-lambda ligand-receptor system: IFN-lambdas exhibit antitumor activity against B16 melanoma. Cancer research. 2006; 66(8):4468–4477. [PubMed: 16618774]
25. Hermant P, Demarez C, Mahlakoiv T, Staeheli P, Meuleman P, Michiels T. Human but not mouse hepatocytes respond to interferon-lambda in vivo. PloS one. 2014; 9(1):e87906. [PubMed: 24498220]
26. Marukian S, Andrus L, Sheahan TP, Jones CT, Charles ED, Ploss A, et al. Hepatitis C virus induces interferon-lambda and interferon-stimulated genes in primary liver cultures. Hepatology. 2011; 54(6):1913–1923. [PubMed: 21800339]
27. Sommereyns C, Paul S, Staeheli P, Michiels T. IFN-lambda (IFN-lambda) is expressed in a tissue-dependent fashion and primarily acts on epithelial cells in vivo. PLoS pathogens. 2008; 4(3):e1000017. [PubMed: 18369468]
28. Pott J, Mahlakoiv T, Mordstein M, Duerr CU, Michiels T, Stockinger S, et al. IFN-lambda determines the intestinal epithelial antiviral host defense. Proceedings of the National Academy of Sciences of the United States of America. 2011; 108(19):7944–7949. [PubMed: 21518880]
29. de Macedo FC, Nicol AF, Cooper LD, Yearsley M, Pires AR, Nuovo GJ. Histologic, viral, and molecular correlates of dengue fever infection of the liver using highly sensitive immunohistochemistry. Diagnostic molecular pathology : the American journal of surgical pathology, part B. 2006; 15(4):223–228.
30. Bierne H, Travier L, Mahlakoiv T, Tailleux L, Subtil A, Lebreton A, et al. Activation of type III interferon genes by pathogenic bacteria in infected epithelial cells and mouse placenta. PloS one. 2012; 7(6):e39080. [PubMed: 22720036]
31. Lebreton A, Lakisic G, Job V, Fritsch L, Tham TN, Camejo A, et al. A bacterial protein targets the BAHD1 chromatin complex to stimulate type III interferon response. Science. 2011; 331(6022): 1319–1321. [PubMed: 21252314]
32. Tamura T, Yanai H, Savitsky D, Taniguchi T. The IRF family transcription factors in immunity and oncogenesis. Annual review of immunology. 2008; 26:535–584.
33. Miyamoto M, Fujita T, Kimura Y, Maruyama M, Harada H, Sudo Y, et al. Regulated expression of a gene encoding a nuclear factor, IRF-1, that specifically binds to IFN-beta gene regulatory elements. Cell. 1988; 54(6):903–913. [PubMed: 3409321]
34. Reis LF, Ruffner H, Stark G, Aguet M, Weissmann C. Mice devoid of interferon regulatory factor 1 (IRF-1) show normal expression of type I interferon genes. The EMBO journal. 1994; 13(20): 4798–4806. [PubMed: 7957048]
35. Stirnweiss A, Ksienzyk A, Klages K, Rand U, Grashoff M, Hauser H, et al. IFN regulatory factor-1 bypasses IFN-mediated antiviral effects through viperin gene induction. J Immunol. 2010; 184(9): 5179–5185. [PubMed: 20308629]
36. Siegel R, Eskdale J, Gallagher G. Regulation of IFN-lambda1 promoter activity (IFN-lambda1/IL-29) in human airway epithelial cells. J Immunol. 2011; 187(11):5636–5644. [PubMed: 22058416]
37. Ueki IF, Min-Oo G, Kalinowski A, Ballon-Landa E, Lanier LL, Nadel JA, et al. Respiratory virus-induced EGFR activation suppresses IRF1-dependent interferon lambda and antiviral defense in airway epithelium. The Journal of experimental medicine. 2013; 210(10):1929–1936. [PubMed: 23999497]
38. Morrison J, Aguirre S, Fernandez-Sesma A. Innate immunity evasion by Dengue virus. Viruses. 2012; 4(3):397–413. [PubMed: 22590678]
39. Stavru F, Bouillaud F, Sartori A, Ricquier D, Cossart P. Listeria monocytogenes transiently alters mitochondrial dynamics during infection. Proceedings of the National Academy of Sciences of the United States of America. 2011; 108(9):3612–3617. [PubMed: 21321208]

NIH-PA Author Manuscript

NIH-PA Author Manuscript

NIH-PA Author Manuscript

40. Koshiba T, Yasukawa K, Yanagi Y, Kawabata S. Mitochondrial membrane potential is required for MAVS-mediated antiviral signaling. Science signaling. 2011; 4(158):ra7. [PubMed: 21285412]
41. Stavru F, Archambaud C, Cossart P. Cell biology and immunology of Listeria monocytogenes infections: novel insights. Immunological reviews. 2011; 240(1):160–184. [PubMed: 21349093]
42. Schrader M, Reuber BE, Morrell JC, Jimenez-Sanchez G, Obie C, Stroh TA, et al. Expression of PEX11beta mediates peroxisome proliferation in the absence of extracellular stimuli. The Journal of biological chemistry. 1998; 273(45):29607–29614. [PubMed: 9792670]
43. Narendra D, Tanaka A, Suen DF, Youle RJ. Parkin is recruited selectively to impaired mitochondria and promotes their autophagy. The Journal of cell biology. 2008; 183(5):795–803. [PubMed: 19029340]
44. Steinberg, SJ.; Raymond, GV.; Braverman, NE.; Moser, AB. Peroxisome Biogenesis Disorders, Zellweger Syndrome Spectrum. In: Pagon, RA.; Bird, TD.; Dolan, CR.; Stephens, K.; Adam, MP., editors. GeneReviews. Seattle (WA): 1993.
45. Eichler F, Van Haren K. Immune response in leukodystrophies. Pediatric neurology. 2007; 37(4): 235–244. [PubMed: 17903666]
46. Waterham HR, Wanders RJ. Metabolic functions and biogenesis of peroxisomes in health and disease. Biochimica et biophysica acta. 2012; 1822(9):1325. [PubMed: 22698677]
47. Halbach A, Landgraf C, Lorenzen S, Rosenkranz K, Volkmer-Engert R, Erdmann R, et al. Targeting of the tail-anchored peroxisomal membrane proteins PEX26 and PEX15 occurs through C-terminal PEX19-binding sites. Journal of cell science. 2006; 119(Pt 12):2508–2517. [PubMed: 16763195]
48. Sacksteder KA, Jones JM, South ST, Li X, Liu Y, Gould SJ. PEX19 binds multiple peroxisomal membrane proteins, is predominantly cytoplasmic, and is required for peroxisome membrane synthesis. The Journal of cell biology. 2000; 148(5):931–944. [PubMed: 10704444]

References for Methods

1. Dixit E, Boulant S, Zhang Y, Lee AS, Odendall C, Shum B, et al. Peroxisomes are signaling platforms for antiviral innate immunity. Cell. 2010; 141(4):668–681. [PubMed: 20451243]
2. Hollinshead M, Sanderson J, Vaux DJ. Anti-biotin antibodies offer superior organelle-specific labeling of mitochondria over avidin or streptavidin. The journal of histochemistry and cytochemistry : official journal of the Histochemistry Society. 1997; 45(8):1053–1057. [PubMed: 9267466]
3. Lencer WI, Delp C, Neutra MR, Madara JL. Mechanism of cholera toxin action on a polarized human intestinal epithelial cell line: role of vesicular traffic. The Journal of cell biology. 1992; 117(6):1197–1209. [PubMed: 1318883]
4. McLaughlin-Drubin ME, Munger K. Biochemical and functional interactions of human papillomavirus proteins with polycomb group proteins. Viruses. 2013; 5(5):1231–1249. [PubMed: 23673719]
5. Warke RV, Becerra A, Zawadzka A, Schmidt DJ, Martin KJ, Giaya K, et al. Efficient dengue virus (DENV) infection of human muscle satellite cells upregulates type I interferon response genes and differentially modulates MHC I expression on bystander and DENV-infected cells. The Journal of general virology. 2008; 89(Pt 7):1605–1615. [PubMed: 18559930]
6. Furlong DB, Nibert ML, Fields BN. Sigma 1 protein of mammalian reoviruses extends from the surfaces of viral particles. Journal of virology. 1988; 62(1):246–256. [PubMed: 3275434]
7. Sabin AB. Research on dengue during World War II. The American journal of tropical medicine and hygiene. 1952; 1(1):30–50. [PubMed: 14903434]
8. Lambeth CR, White LJ, Johnston RE, de Silva AM. Flow cytometry-based assay for titrating dengue virus. Journal of clinical microbiology. 2005; 43(7):3267–3272. [PubMed: 16000446]
9. Gouin E, Mengaud J, Cossart P. The virulence gene cluster of Listeria monocytogenes is also present in Listeria ivanovii, an animal pathogen, and Listeria seeligeri, a nonpathogenic species. Infection and immunity. 1994; 62(8):3550–3553. [PubMed: 8039927]

NIH-PA Author Manuscript

NIH-PA Author Manuscript

NIH-PA Author Manuscript

10. Lebreton A, Lakisic G, Job V, Fritsch L, Tham TN, Camejo A, et al. A bacterial protein targets the BAHD1 chromatin complex to stimulate type III interferon response. Science. 2011; 331(6022): 1319–1321. [PubMed: 21252314]

11. Amit I, Garber M, Chevrier N, Leite AP, Donner Y, Eisenhaure T, et al. Unbiased reconstruction of a mammalian transcriptional network mediating pathogen responses. Science. 2009; 326(5950): 257–263. [PubMed: 19729616]

NIH-PA Author Manuscript
NIH-PA Author Manuscript
NIH-PA Author Manuscript

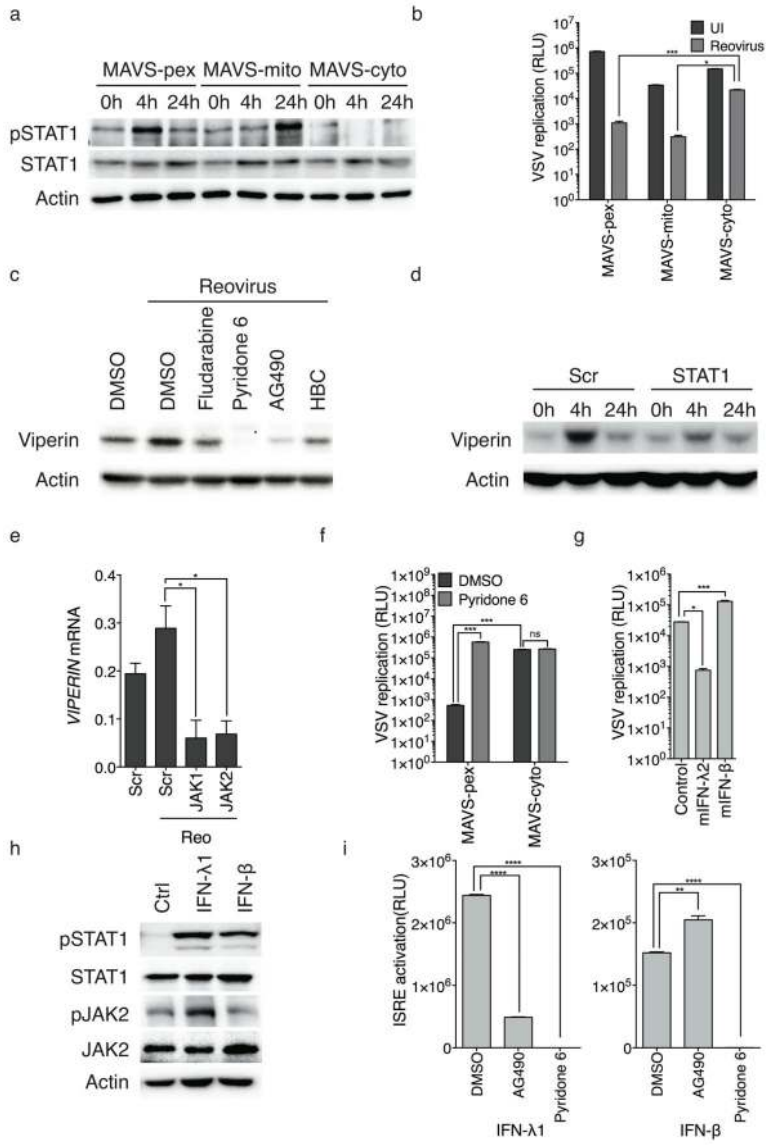

Fig. 1. Peroxisomal MAVS induces JAK/STAT-dependent antiviral responses that have characteristics of Type III IFN signaling

(a) MAVS-KO MEFs expressing MAVS alleles localized exclusively on peroxisomes (Pex), mitochondria (Mito) or in the cytosol (Cyto) were infected with reovirus. At indicated times, cell culture media were collected and incubated with Huh7.5 cells. STAT1 phosphorylation was assessed by western immunoblotting with a phosphospecific antibody. (b) Similarly to (a) except Huh7.5 cells were subsequently infected with VSV expressing firefly Luciferase. Luciferase expression was used as a measure of viral replication. (c) MAVS-KO MEFs expressing MAVS-Pex were treated with 50 μM Fludarabine, 2 μM Pyridone 6, 50 μM AG490 or 50 μM HBC, and infected with reovirus for 4h. Expression of the ISG viperin was determined by immunoblotting. (d) MAVS-KO MEFs expressing MAVS-pex were depleted of STAT1 and infected with reovirus for the times indicated. Viperin expression was determined. (e) JAK1 or JAK2 were knocked down in MAVS-KO MEFs expressing MAVS-Pex, which were subsequently infected with reovirus for 4h. *VIPERIN* mRNA

NIH-PA Author Manuscript

NIH-PA Author Manuscript

NIH-PA Author Manuscript

expression was quantified by qRT-PCR. (f) Similarly to (c), MAVS-Pex MEFs were treated with the pan-JAK inhibitor Pyridone 6 and infected with VSV expressing firefly luciferase (VSV). Luciferase expression was used as a measure of viral replication. (g) Huh7.5 cells were incubated with mouse IFN-λ2 or IFN-β and subsequently infected with VSV. (h) Huh7.5 cells were treated with human IFN-λ1 or IFN-β for 2 h. STAT1 and JAK2 phosphorylation levels were determined by western immunoblotting using phosphospecific antibodies. (i) 293T cells expressing Luciferase under the control of an ISRE promoter were treated with the JAK2 inhibitor AG490 or the pan-JAK inhibitor Pyridone 6. Cells were then incubated with human IFN-λ1 or IFN-β and assessed for their ability to respond to IFNs by producing luciferase.

Error bars represent mean ± SD (b, f, g, i) or SEM (e) of triplicate readings for one experiment representative of 3. *, $P<0.05$; **, $P < 0.01$; ***, $P < 0.0001$ (One-way ANOVA).

NIH-PA Author Manuscript

NIH-PA Author Manuscript

NIH-PA Author Manuscript

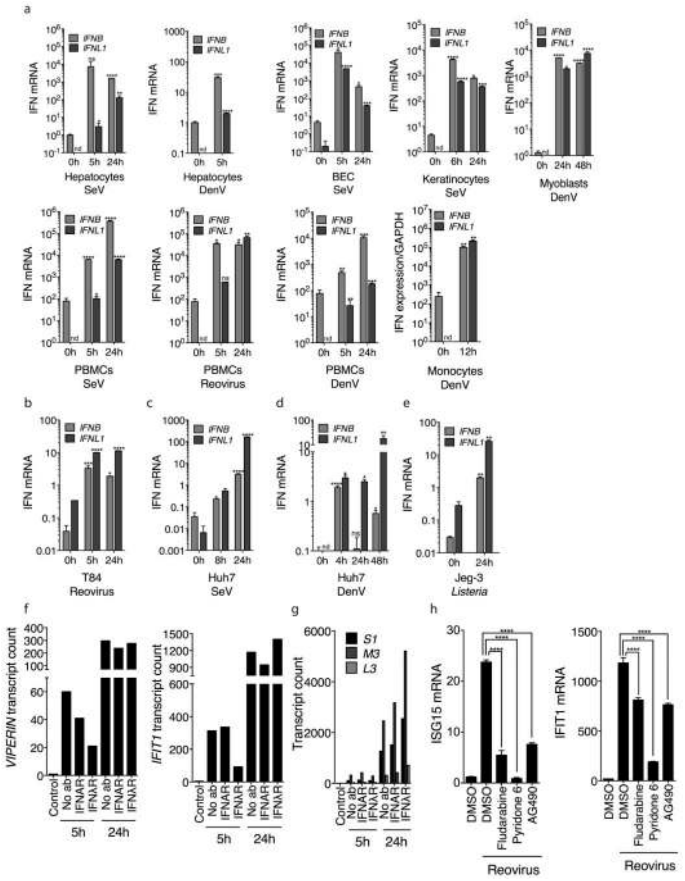

Fig. 2. Type III IFNs are produced during viral infections and are important for the antiviral functions of human cells

(a) Primary epithelial and stromal cells were infected with the indicated viruses for the times shown. qRT-PCR was carried out to determine *IFNL1* and *IFNB* mRNA expression. (b) Polarized T84 epithelial cells were infected with reovirus for the indicated times. *IFNB* or *IFNL1* mRNA expression was assessed by qRT-PCR. (c–d) Huh7 cells were infected with SeV (c) or DenV (d) for the indicated time points. *IFNB* or *IFNL1* mRNA expression were assessed by qRT-PCR. (e) JEG3 trophoblasts were infected with *Listeria monocytogenes*. *IFNB* or *IFNL1* mRNA expression was assessed by qRT-PCR. (f) Polarized T84 cells were pre-incubated with neutralizing antibodies against the type I IFN receptor (IFNAR) or the Type III IFN receptor (IFNλR). Cells were then infected for the indicated times and ISG mRNA expression was determined by nCounter. (g) Similar to (f) except reovirus gene expression was analyzed. (h) Polarized T84 cells were pre-incubated with 10–50 μM Fludarabine, 2 μM Pyridone 6 or 10–50 μM AG490. Cells were infected with reovirus and assessed for mRNA expression of the ISGs *IFIT1* and *ISG15* by qRT-PCR. Error bars represent mean ± SEM of triplicate readings for one experiment representative of 2 (a) or 3 (b–h).

*, P<0.05; **, P < 0.01; ***, P < 0.001; ****, P < 0.0001 (One-way ANOVA). Unless otherwise indicated, comparisons were made between uninfected (0h) and infected samples (a–e).

NIH-PA Author Manuscript

NIH-PA Author Manuscript

NIH-PA Author Manuscript

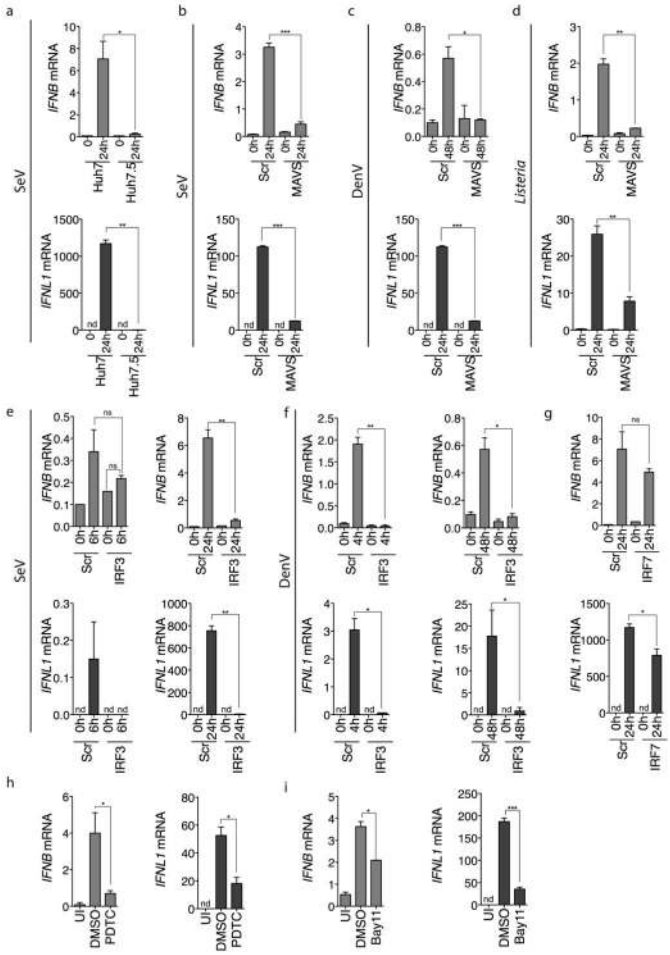

Fig. 3. Similarities between Type I and Type III IFN regulation

(a) Huh7 or Huh7.5 cells were infected with SeV. At the indicated time point, RNA was isolated and *IFNB* or *IFNL1* mRNA expression was determined by qRT-PCR. (b–c) Huh7 cells were transfected with a scrambled (Scr) or MAVS siRNA oligo, and subsequently infected with SeV (b) or DenV (c) for 24h. *IFNB* or *IFNL1* mRNA expression were determined by qRT-PCR. (d) Similar to (b) except JEG3 cells were infected with *Listeria monocytogenes.* (e–f) Cells were transfected with a scrambled (Scr) or IRF3 siRNA and infected with SeV (e) or DenV (f) for the times indicated. *IFNB* or *IFNL1* mRNA expression was determined by qRT-PCR. (g) Similar to (e) except cells were depleted of IRF7. (h–i) Huh7 cells were treated with the NFκB inhibitors Pyrrolidinedithiocarbamate Ammonium (PDTC, h), or Bay11 (i) and infected with SeV. *IFNB* or *IFNL1* mRNA expression was determined by qRT-PCR. Error bars represent mean ± SEM of triplicate readings for one experiment representative of 3 (h, i), 4 (a–d) or 5 (e–g).

*, P<0.05; **, P < 0.01; ***, P < 0.001 (Student's *t*-test).

NIH-PA Author Manuscript

NIH-PA Author Manuscript

NIH-PA Author Manuscript

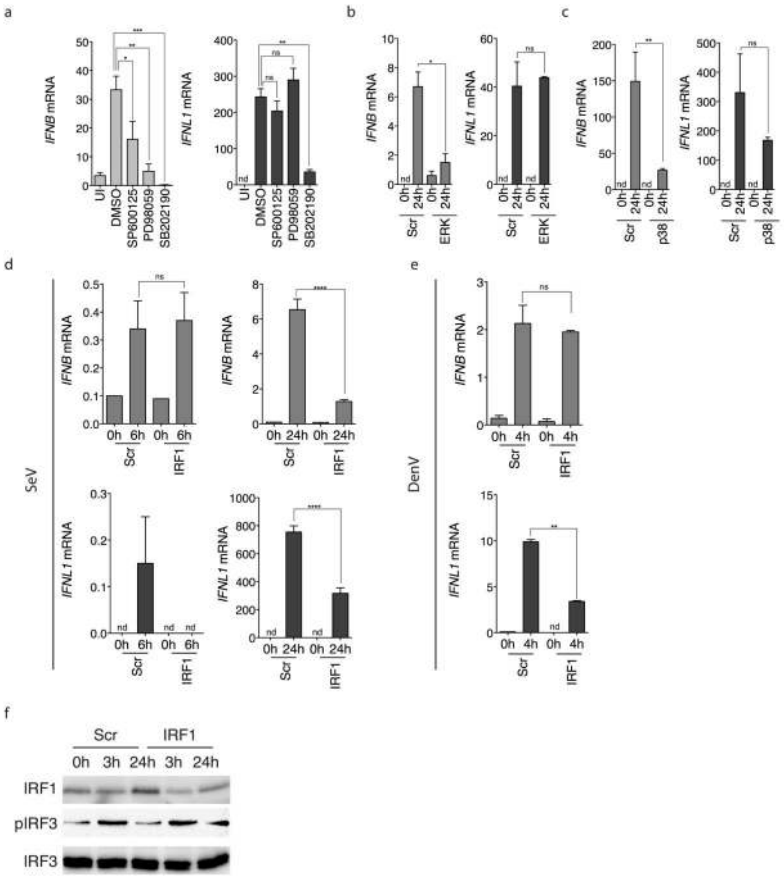

Fig. 4. IFN-λ1 is regulated by a unique pathway that involves IRF1

(a) Huh7 hepatocytes were treated with MAP kinase inhibitors targeting JNK (SP600125), MEK/ERK (PD98059) and p38 (SB202190). Following SeV infection, *IFNB* and *IFNL1* mRNA expression was determined by qRT-PCR. (b) ERK or (c) p38 were knocked down in Huh7 cells, and then infected overnight with SeV. *IFNB* or *IFNL1* mRNA expression was determined by qRT-PCR. (D–E) IRF1 was knocked down in Huh7 cells that were subsequently infected with SeV (d) or DenV (e) for the times indicated. *IFNB* or *IFNL1* mRNA expression was determined by qRT-PCR. (f) IRF1 was knocked down in Huh7 cells that were subsequently infected with SeV for 3 and 24h. IRF3 phosphorylation was visualized by western immunoblotting using a phosphospecific antibody. Error bars represent mean ± SEM of triplicate readings for one experiment representative of 2 (a–c) or 3 (d–e).

*, P<0.05; **, P < 0.01; ***, P < 0.001; ****, P < 0.0001 (One-way ANOVA (a) or Student's *t*-test (b–e)).

NIH-PA Author Manuscript

NIH-PA Author Manuscript

NIH-PA Author Manuscript

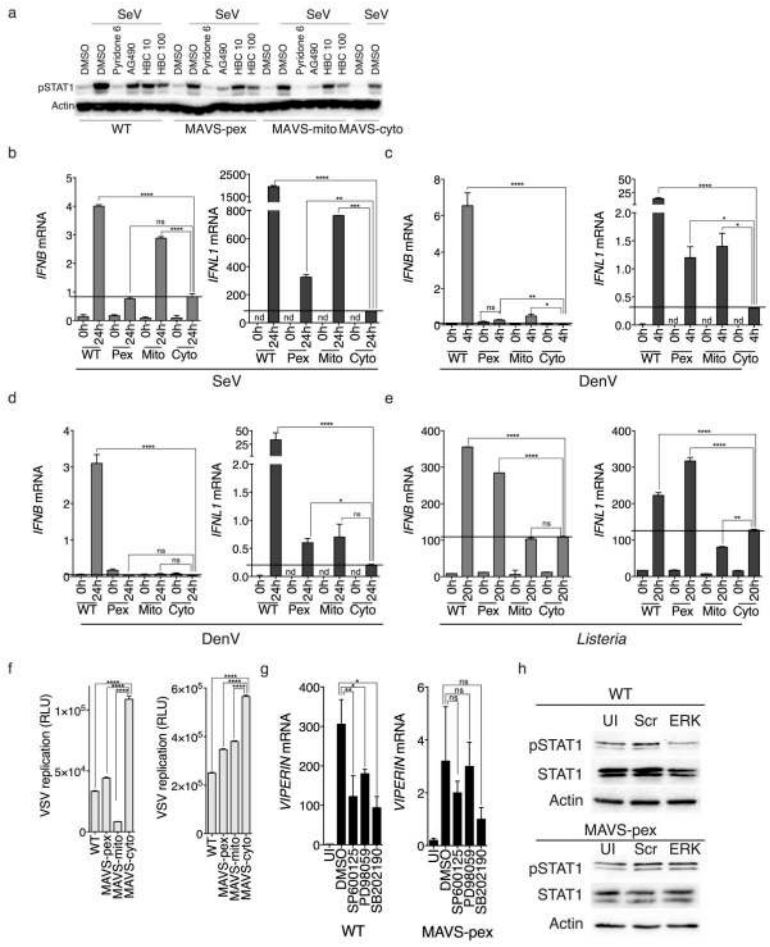

Fig. 5. Peroxisomal MAVS selectively induces Type III IFNs

(a) Huh7 cells stably expressing wild-type MAVS (WT), peroxisomal MAVS (Pex), mitochondrial MAVS (Mito) or cytoplasmic MAVS (Cyto) were depleted of endogenous MAVS. Cells were then incubated with 2 μM Pyridone 6, 50 μM AG490 or 10–100 μM HBC, and infected with SeV (SeV). STAT1 phosphorylation (pSTAT1) was assessed by western analysis. (b–d) Huh7 cells expressing MAVS transgenes were depleted of endogenous MAVS and infected with SeV (b) or DenV (c–d) for the time points indicated. *IFNB* or *IFNL1* mRNA expression was determined by qRT-PCR. (e) JEG3 trophoblasts were transfected with plasmids encoding the MAVS alleles indicated and subsequently infected with *Listeria monocytogenes*. *IFNB* or *IFNL1* mRNA expression was determined by qRT-PCR. (f) Cell culture supernatants from (b) or (d) were incubated with Huh7.5 cells that were subsequently infected with luciferase-expressing Vesicular Stomatitis Virus (VSV). Luciferase expression was used as a measure of viral replication. (g) Huh7 hepatocytes expressing WT or MAVS-pex were depleted of endogenous MAVS and were treated with MAP kinases inhibitors targeting JNK (SP600125), MEK and ERK (PD98059) and p38 (SB202190). Following SeV infection, *VIPERIN* mRNA expression was determined by qRT-PCR. (h) MAVS-KO MEFs expressing WT MAVS (top panel) or MAVS-pex (bottom panel) were infected with reovirus for 4h. STAT1 phosphorylation was measured by western immunoblotting with a phosphospecific antibody. Error bars represent

mean ± SEM of triplicate readings for one experiment representative of 2 (g), 3 (c–f) or 5 (b).

*, P<0.05; **, P < 0.01; ****, P < 0.0001 (One-way ANOVA).

NIH-PA Author Manuscript
NIH-PA Author Manuscript
NIH-PA Author Manuscript

NIH-PA Author Manuscript

NIH-PA Author Manuscript

NIH-PA Author Manuscript

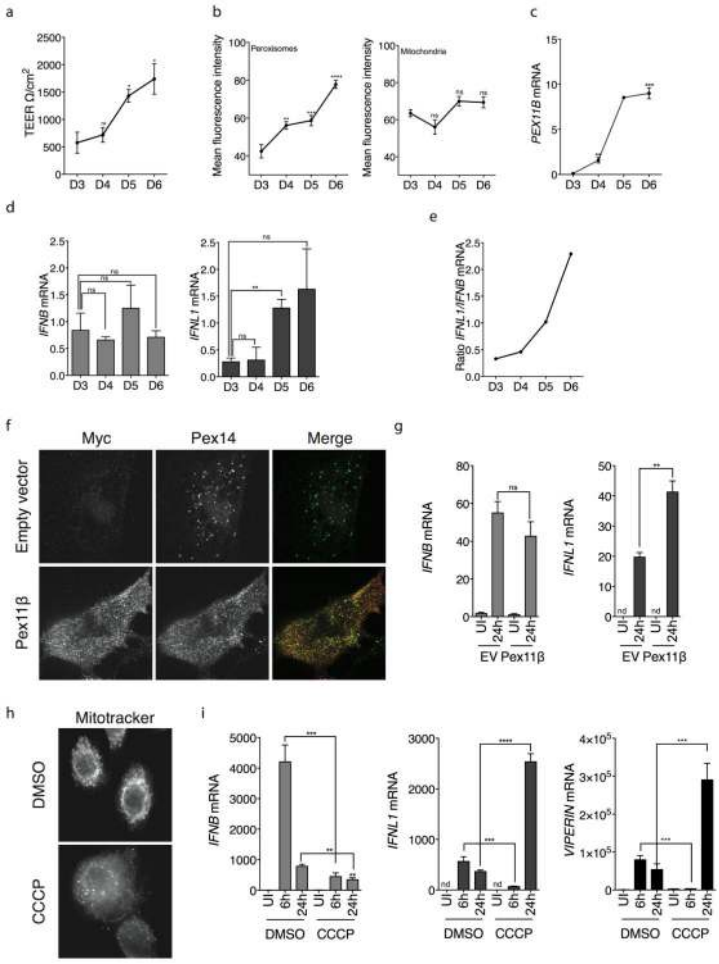

Fig. 6. The abundance and function of mitochondria and peroxisomes affects the quality of the IFN response

(a) T84 colonic epithelial cells were allowed to polarize on transwells. Transepithelial electrical resistance of T84 epithelial cells was measured between Day 3 and Day 6 after plating (D3–D6). (b) Peroxisome (left panel) and Mitochondria (right panel) were visualized in polarizing T84 cells. Peroxisome or Mitochondria abundance was quantified by densitometric analyses of multiple images. (c) During T84 cell polarization, *Pex11B* mRNA expression was quantified by qRT-PCR. (d) T84 cells were infected every day for 24h with reovirus, and *IFNB* or *IFNL1* mRNA levels were measured by qRT-PCR. (e) The ratio of *IFNB* or *IFNL1* mRNA induced by reovirus infection was plotted over time. (f) Huh7 hepatocytes expressing the peroxisome biogenesis regulator Pex11β were labeled for the peroxisomal marker Pex14. (g) Control (Empty vector, EV) or Pex11β expressing cells were infected with SeV for 24h, IFNs were measured by qRT-PCR. (h) Keratinocytes were treated with DMSO or the mitochondria membrane potential disrupting agent CCCP. Depolarization of mitochondria was visualized by mitotracker staining. (i) CCCP-treated keratinocytes were infected with SeV for the indicated times. *IFNB*, *IFNL1* and *VIPERIN* mRNA expression was determined by qRT-PCR. Micrographs are representative of at least 3 independent experiments where over 500 cells were inspected. Error bars represent mean ± SEM of triplicate readings for one experiment representative of 3.

*, P<0.05; **, P < 0.01; ***, P < 0.0001 (One-way ANOVA). Unless otherwise indicated, comparisons were made between Day 3 (D3) samples and others (a–c).

NIH-PA Author Manuscript
NIH-PA Author Manuscript
NIH-PA Author Manuscript